PNAS RESEARCH ARTICLE | PHARMACOLOGY

Nuclear VCP drives colorectal cancer progression by promoting fatty acid oxidation

Youwei Huang[a,b,c,1], Fang Wang[a,1], Xi Lin[a,1], Qing Li[a], Yuli Lu[a,d], Jiayu Zhang[e], Xi Shen[a], Jingyi Tan[c], Zixi Qin[a], Jiahong Chen[a,f], Xueqin Chen[a], Guopeng Pan[a], Xiangyu Wang[a], Yuequan Zeng[a], Shangqi Yang[a], Jun Liu[a], Fan Xing[g,2], Kai Li[e,2], and Haipeng Zhang[a,2]

Edited by Michael Hall, Universitat Basel, Basel, Switzerland; received December 24, 2022; accepted August 26, 2023

Fatty acid oxidation (FAO) fuels many cancers. However, knowledge of pathways that drive FAO in cancer remains unclear. Here, we revealed that valosin-containing protein (VCP) upregulates FAO to promote colorectal cancer growth. Mechanistically, nuclear VCP binds to histone deacetylase 1 (HDAC1) and facilitates its degradation, thus promoting the transcription of FAO genes, including the rate-limiting enzyme *carnitine palmitoyltransferase 1A* (*CPT1A*). FAO is an alternative fuel for cancer cells in environments exhibiting limited glucose availability. We observed that a VCP inhibitor blocked the upregulation of FAO activity and CPT1A expression triggered by metformin in colorectal cancer (CRC) cells. Combined VCP inhibitor and metformin prove more effective than either agent alone in culture and in vivo. Our study illustrates the molecular mechanism underlying the regulation of FAO by nuclear VCP and demonstrates the potential therapeutic utility of VCP inhibitor and metformin combination treatment for colorectal cancer.

fatty acid oxidation | VCP | colorectal cancer | metformin | combination therapy

Significance

Multiple cancer types, especially some certain types of cancers which proximity to the adipose tissue, have been suggested to rely on fatty acid oxidation (FAO) for survival. However, the mechanism by which FAO is regulated in tumors remains elusive. Here, using transcriptomic and metabolomic analyses, we discover the previously unknown role of valosin-containing protein (VCP) in regulating FAO in colorectal cancer (CRC). Moreover, we created a concept of combination therapy consisting of VCP inhibitors and metformin, which would be particularly effective for the treatment of CRCs. This study offers insight into mechanisms that drive fatty acid addiction in CRC and provides a rationale for clinical studies directed at exploring VCP inhibitors in combination with metformin in the treatment of CRC.

Rewiring cellular metabolism is crucial for sustaining the increased growth and proliferation of tumors. Although numerous studies have reported the use of glucose and glutamine by tumor cells, a number of cancers prefer to metabolize fats (1). Obesity is a risk factor for at least 13 types of cancers, including colorectal cancer (CRC) (2, 3). More recent studies examining colon and breast cancer suggest that cancer cells possess a clear predilection for spreading to adipocyte-rich tissues (4, 5). The uptake of fatty acids from surrounding adipocytes promotes fatty acid oxidation (FAO) in cancer cells (4, 6). FAO is an alternative source of energy for multiple cancer types and provides raw materials for the tricarboxylic acid (TCA) cycle to produce ATP (7). FAO is involved in the production of cytosolic nicotinamide adenine dinucleotide phosphate (NADPH) where it reduces the power to support biosynthesis and counteracts oxidative stress (8). Although multiple cancer types have been reported to rely on FAO for proliferation, survival, stemness, drug resistance, or metastasis (9–11), knowledge regarding the pathways that drive FAO in the context of cancer remains limited. Therefore, it is critical to understand the molecular mechanism underlying FAO regulation in tumors, as this is important for the improvement of metabolism-targeted cancer therapy and its subsequent clinical effects.

Valosin-containing protein (VCP), also known as P97, is a central component of the ubiquitin-proteasome degradation system (UPS) (12). VCP forms a complex with cofactors that typically enhance the efficiency of ubiquitin binding and define substrate and pathway selection (13). Augmented VCP expression correlates with poor prognosis for certain cancers, including colorectal cancer (14), gastric carcinoma (15), and hepatocellular carcinoma (16). Targeting VCP to disrupt cellular proteostasis represents an attractive strategy for cancer therapy (17–19). Previous work on the role of VCP in cancer has largely focused on its cytoplasmic functions, primarily the endoplasmic reticulum-associated degradation (ERAD) pathway (18, 20). However, recent research has also defined VCP as a central player in various chromatin-associated processes (21, 22). These findings uncover the roles of VCP in fundamental chromatin-associated processes and indicate that there are probably more to be explored. Recently, VCP was reported to regulate glutamine metabolism by disassembling the glutamine synthetase oligomer to promote its degradation (23); however, its role in regard to tumor lipid metabolism is unclear.

The study examining FAO in the context of cancer metabolism has unveiled new and exciting therapeutic opportunities, whereas targeting single pathways rarely results in a definitive cure for cancers (8). Thus, it is likely that agents that target FAO will need to be combined with other targeting agents for successful treatment of cancer. FAO has been demonstrated to contribute to mitochondrial spare respiratory capacity that is the extra capacity of cells to produce energy under conditions of increased stress (24). Previous studies have demonstrated that treatment with metformin promotes fatty acid oxidation to fuel the TCA cycle in environments with limited glucose availability (25–27). As such,

Author contributions: F.X., K.L., and H.Z. designed research; Y.H., F.W., X.L., Q.L., Y.L., J.Z., X.S., J.T., Z.Q., J.C., X.C., G.P., X.W., Y.Z., S.Y., J.L., and H.Z. performed research; Y.H., F.W., X.L., and H.Z. analyzed data; and Y.H. and H.Z. wrote the paper.

The authors declare no competing interest.

This article is a PNAS Direct Submission.

[1]Y.H., F.W. and X.L. contributed equally to this work.

[2]To whom correspondence may be addressed. Email: zhanghp@jnu.edu.cn, likai39@mail.sysu.edu.cn, or xingfan@gdph.org.cn.

This article contains supporting information online at https://www.pnas.org/lookup/suppl/doi:10.1073/pnas.2221653120/-/DCSupplemental.

Published October 3, 2023.

we hypothesized that the increased reliance on FAO may affect the survival of metformin-treated cells and thus confer a unique vulnerability, which provides evidence for exploring combinatorial strategies of small molecules targeting FAO and metformin in cancer treatment.

In this study, we investigate how nuclear VCP, a key component of the UPS, regulates FAO in CRC cells. Moreover, our study revealed that a VCP inhibitor abrogated the up-regulated FAO activity induced by metformin. Consequently, a combined treatment using a VCP inhibitor with metformin significantly suppressed tumor growth in CRC tumors and in patient-derived xenograft (PDX) models compared with single-agent. These findings clarify the previously unknown role of VCP in regulating fatty acid metabolism and provide an efficient therapeutic combination for the treatment of CRCs.

Results

Nuclear VCP Promotes CRC Growth. Analyses using The Cancer Genome Atlas (TCGA) and Gene Expression Omnibus (GEO) databases revealed that VCP expression was elevated in multiple cancer types, including colorectal cancer, which correlates with poor clinical outcome in patients (*SI Appendix*, Fig. S1 *A* and *B*). Overexpression of VCP significantly promoted CRC growth both in vitro and in vivo (*SI Appendix*, Fig. S1 *C–I*). However, the role of VCP in the malignant progression of CRC remains unclear. VCP has been extensively studied in the context of the ERAD, a process that is required for the extraction of misfolded proteins from the ER membrane (12). Therefore, we first evaluated whether the cellular functions of VCP in the ERAD pathway play key roles in promoting CRC growth. As the Sel1L–Hrd1 protein complex constitutes the most conserved form of ERAD (28), we established an ERAD-deficient model through the use of CRISPR/Cas9-mediated knockout of Sel1L in CRC cells, and we explored whether ERAD deficiency affects VCP-promoted CRC growth. IRE1α is an endogenous ERAD substrate in vitro (29), and deletion of Sel1L increased IRE1α protein level (*SI Appendix*, Fig. S2*A*). We next overexpressed VCP in Sel1L-deficient CRC cells (*SI Appendix*, Fig. S2*B*), and we observed that overexpression of VCP promoted tumor cell growth in the ERAD-deficient model compared to that in the vector group (*SI Appendix*, Fig. S2 *C–F*). These data indicate that other functions of VCP may be more critical for CRC growth.

VCP was also highly expressed in the nuclei of CRC cells (Fig. 1 *A* and *B*). Thus, we deleted the nuclear localization sequence (NLS) of VCP to generate the $VCP^{\Delta NLS}$ mutant protein as previously described (30), and we confirmed that the $VCP^{\Delta NLS}$ mutant protein failed to enter the nucleus (Fig. 1 *C–E*). Interestingly, we found that exogenous $VCP^{\Delta NLS}$ mutant protein was unable to promote CRC growth compared to the VCP group as judged by cell viability assay, colony formation assay, and 5-ethynyl-2′deoxyuridine (EdU) staining (Fig. 1 *F–I*). Together, these observations suggest that nuclear VCP plays a key role in promoting CRC growth.

VCP Regulates FAO in CRC. Considering that VCP can regulate chromatin-associated processes, we first performed RNA sequencing to investigate the global gene expression profiles in CRC cells expressing VCP or a control vector. Gene set enrichment analysis (GSEA) between experimental groups revealed significant upregulation of genes that regulate fatty acid metabolism and fatty acid β-oxidation processes in cells undergoing VCP overexpression (Fig. 2*A*). Further analysis revealed that VCP overexpression up-regulated the transcription of multiple key genes in the FAO pathway, including the rate-limiting enzyme *CPT1A* (Fig. 2*B*). To confirm our gene array data, we detected the transcription of key FAO genes using qPCR. As the data showed, overexpression of VCP significantly increased the expression of FAO genes (Fig. 2*C*), while silencing VCP with dox-inducible shRNA down-regulated the expression of these genes (Fig. 2*D*). These data demonstrated that VCP transcriptionally regulates FAO. Finally, analyses using TCGA datasets revealed that *VCP* expression positively correlated with *CPT1A* expression in various cancer types including CRC (*SI Appendix*, Fig. S3).

Acylcarnitines are essential intermediates involved in the first committed step of FAO (31, 32). To catabolize long-chain fatty acids (such as palmitate) to acetyl–coenzyme A (acetyl-CoA) that act as a major fuel for biosynthetic and bioenergetic metabolism, acyl-CoAs must be enzymatically converted to acylcarnitines across the outer mitochondrial membrane by CPT1 (8). Using a targeted metabolomics approach, we further confirmed that the FAO intermediates, including long-acylcarnitine C25:2 and most medium- and short-chain acylcarnitines, were dramatically increased in VCP-overexpressing CRC cells (Fig. 2*E*). In contrast, VCP knockdown decreased the concentrations of short-chain C9:2 and long-acylcarnitines (Fig. 2*F*). Collectively, these findings indicate that VCP can regulate FAO by affecting the transcription of FAO genes.

Nuclear VCP Promotes FAO in CRC. FAO requires the rate-limiting enzyme CPT1 to transport lipids into the mitochondria (33). We observed increased protein levels of CPT1A in VCP-overexpressing CRC cells, and this was consistent with the mRNA results described above (Fig. 3*A*). However, $VCP^{\Delta NLS}$ induced a smaller increase in CPT1A expression compared to that observed in VCP-overexpressing cells (Fig. 3*A*). Acceleration of fatty acid catabolism typically causes lipid content reduction in the cytoplasm in the form of adiposomes due to increased fatty acid utilization. Thus, we assessed the lipid droplet contents to determine the role of VCP in FAO regulation. Notably, VCP overexpression resulted in reduced lipid droplet contents in CRC cells, while cells expressing $VCP^{\Delta NLS}$ exhibited significantly higher levels of adiposomes than did the cells in VCP group (Fig. 3 *B* and *C*), thus suggesting that nuclear VCP is critical for promoting fatty acid utilization.

FAO is the primary bioenergetic pathway that produces ATP and NADPH (8). Therefore, we investigated the effect of VCP on ATP and NADPH production. Our data revealed that overexpression of VCP significantly increased ATP and NADPH production, while $VCP^{\Delta NLS}$ induced a smaller increase in ATP and NADPH production compared to that observed in VCP-overexpressing cells (*SI Appendix*, Fig. S4 *A* and *B*). We next examined the metabolic fate of palmitate by tracing ^{13}C-labeled palmitate and found VCP overexpression notably increased M + 2 citrate as well as other TCA metabolites, highlighting that exogenous VCP promotes incorporation of carbons derived from palmitate into TCA cycle (Fig. 3 *D* and *E*). Furthermore, we measured the oxygen consumption rate (OCR) in response to etomoxir, a well-known FAO inhibitor targeting CPT1 (34). We observed that VCP-overexpressing CRC cells exhibited a higher overall OCR than did the vector cells (*SI Appendix*, Fig. S4*C*). Importantly, the Eto-sensitive OCR in the VCP-overexpressing cells was significantly higher than that in the vector group, thus suggesting an increase in FAO activity that was mediated by VCP overexpression (Fig. 3 *F* and *G*). Meanwhile, cells expressing $VCP^{\Delta NLS}$ exhibited lower Eto-sensitive OCR compared to the VCP-overexpression group, thus indicating that nuclear VCP contributes to the increased activity of FAO (Fig. 3 *H* and *I* and *SI Appendix*, Fig. S4*D*). Additionally, cells transfected with either VCP or vector showed enhanced OCR capacity in palmitate

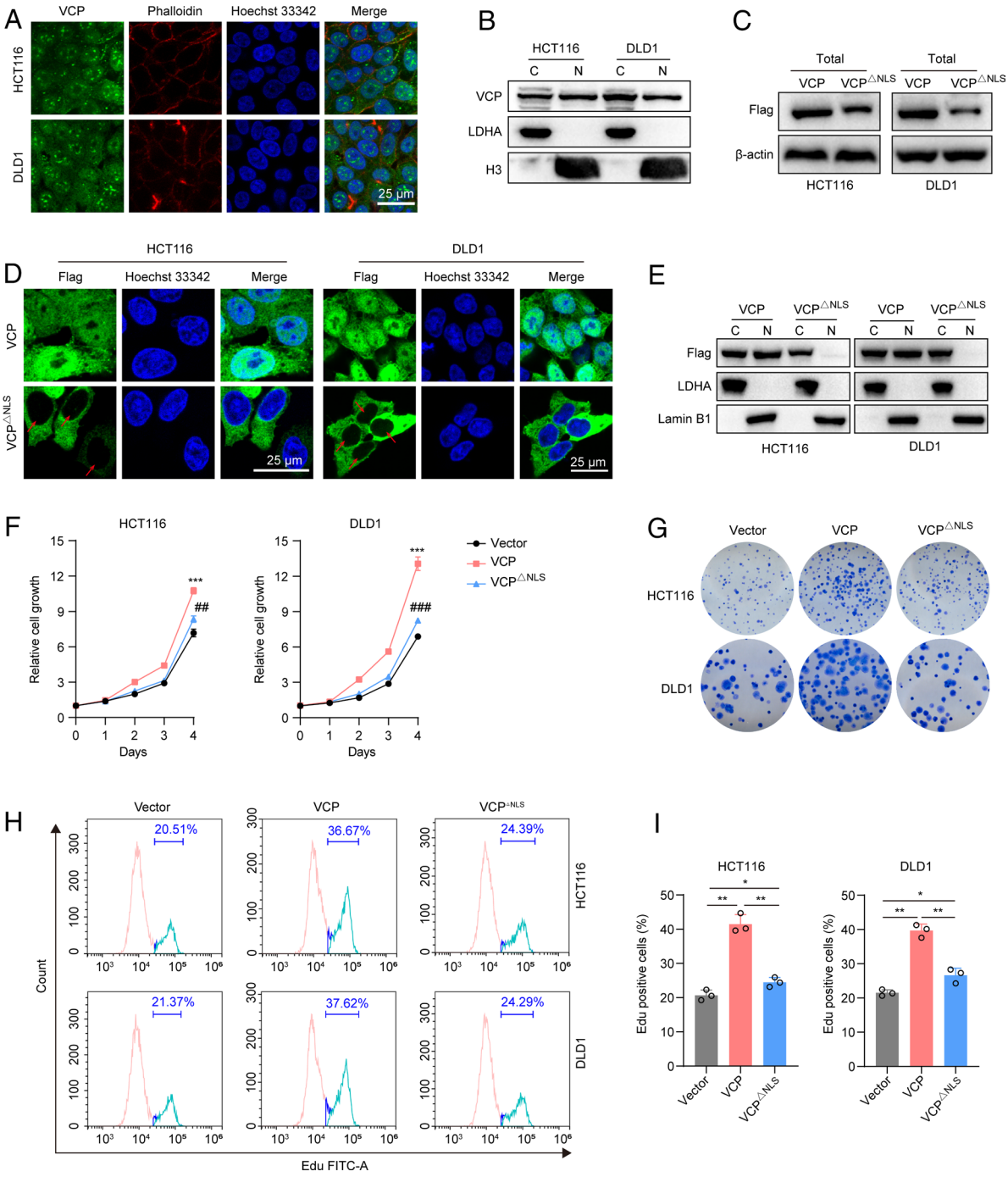

Fig. 1. Nuclear VCP promotes CRC growth. (*A*) Immunofluorescent staining of VCP (green) in HCT116 and DLD1 cells. The cytoplasm was stained with phalloidin (red), and nuclei were stained with Hoechst 33342 (blue) (Scale bar, 25 μm). (*B*) Western blot analysis assessing the distribution of VCP in the cytosolic (C) and nuclear (N) fractions. LDHA and H3 were used as cytoplasmic and nuclear markers, respectively. (*C*) Western blot analysis of Flag-VCP in cells stably expressing Flag-tagged VCP or VCP$^{\triangle NLS}$. (*D*) Immunofluorescent staining for Flag (green) and Hoechst 33342 (blue) in cells stably expressing Flag-tagged VCP or VCP$^{\triangle NLS}$. Red arrows depict the nuclear VCP localization (Scale bar, 25 μm). (*E*) Western blot analysis of Flag-VCP in the cytosolic and nuclear fractions of the indicated cells stably expressing Flag-tagged VCP or VCP$^{\triangle NLS}$. LDHA and Lamin B1 were used as cytoplasmic and nuclear markers, respectively. (*F*) The relative growth of HCT116 and DLD1 cells stably expressing VCP, VCP$^{\triangle NLS}$, or control vector, $n = 3$. *: VCP versus vector at day 4, #: VCP$^{\triangle NLS}$ versus VCP at day 4. (*G*) Colony formation assay of HCT116 and DLD1 cells stably expressing VCP, VCP$^{\triangle NLS}$, or control vector, $n = 3$. (*H* and *I*) Flow cytometry analysis of EdU incorporation and PI staining of cells stably expressing VCP, VCP$^{\triangle NLS}$, or control vector. (*I*) EdU-positive cells were quantified, $n = 3$. Data represent the mean ± SD. $^{*}P < 0.05$, $^{**}P$ or $^{\#\#}P < 0.01$, $^{***}P$ or $^{\#\#\#}P < 0.001$. *P* values were determined by one-way ANOVA. See also *SI Appendix*, Figs. S1 and S2.

(PAM)-containing medium compared to that in the control medium (*SI Appendix*, Fig. S4*E*). Nevertheless, VCP-overexpressing cells exhibited higher PAM-inducible OCR than did control cells (Fig. 3 *J* and *K*). In particular, the increase in PAM-inducible OCR in cells transfected with VCP$^{\Delta NLS}$ was attenuated compared to that in the VCP-overexpressing cells, further demonstrating that the increased FAO capacity was due to the nuclear VCP (Fig. 3 *L* and *M* and *SI Appendix*, Fig. S4*F*).

To date, there is little information regarding the role of VCP in driving cancer progression by regulating tumor lipid metabolism. We next examined whether the promotion of cell growth caused by elevated VCP levels in CRC is dependent upon FAO.

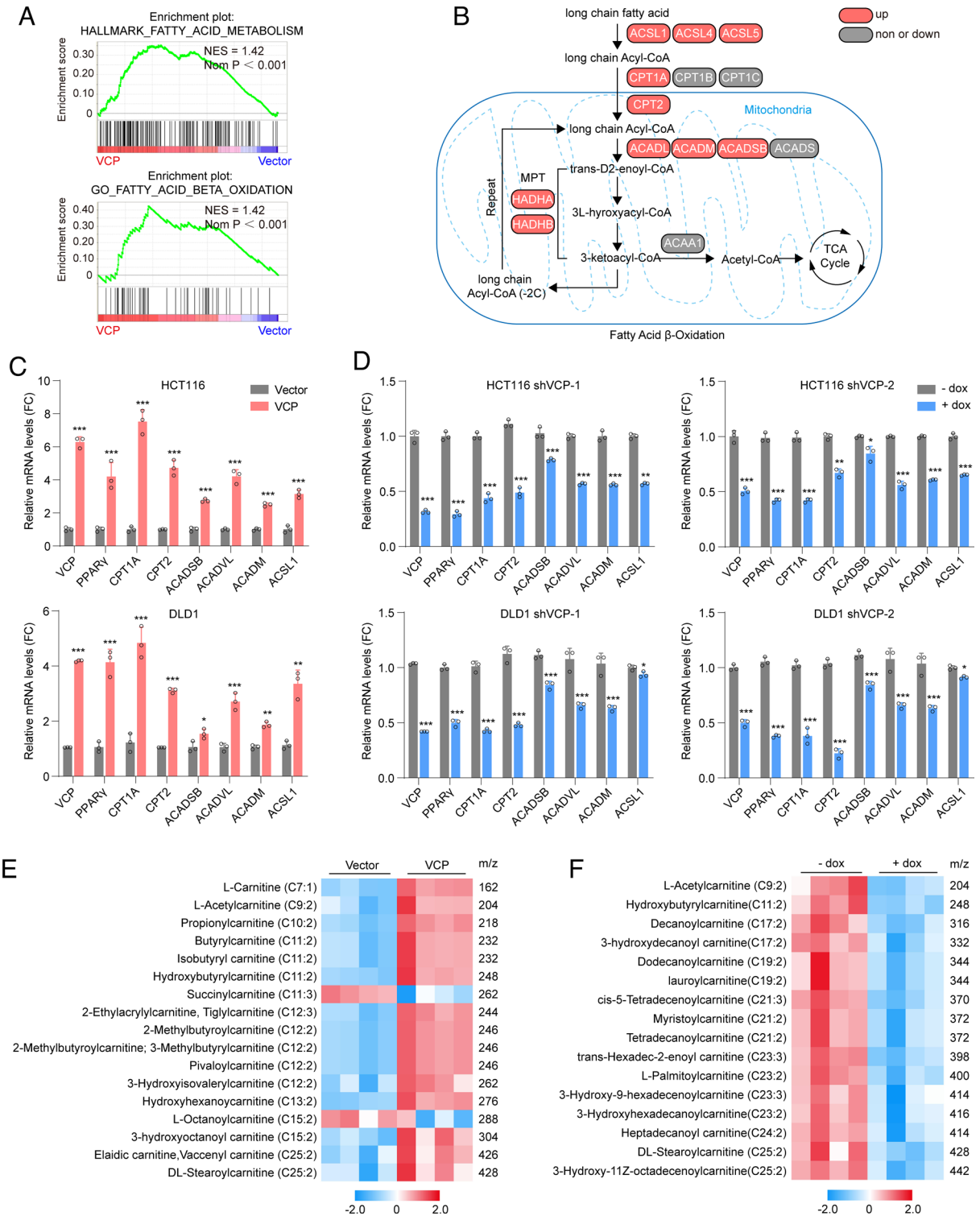

Fig. 2. VCP regulates FAO in CRC. (*A*) GSEA using genes differentially expressed between HCT116 cells stably expressing VCP or control vector. (*B*) Pathway map presenting changes in transcript levels of FAO genes in VCP-overexpressed cells relative to control cells. (*C*) qPCR analysis assessing expression of FAO genes in cells stably expressing VCP or control vector, $n = 3$. (*D*) qPCR analysis assessing expression of FAO genes in cells transfected with dox-inducible shVCP in the absence or presence of dox, $n = 3$. (*E* and *F*) Targeted metabolomics analysis of acylcarnitines in HCT116 cells under different treatments. (*E*) HCT116 cells stably expressing VCP or control vector, $n = 4$. (*F*) HCT116 cells were transfected with dox-inducible shVCP in the absence or presence of dox, $n = 4$. Data represent the mean ± SD in (*C* and *D*) or mean ± SEM in (*E* and *F*). $^{*}P < 0.05$; $^{**}P < 0.01$; $^{***}P < 0.001$. *P* values were determined by Student's *t* test. See also *SI Appendix*, Fig. S3.

Our data showed that the increased clonogenic capacity induced by exogenous VCP was significantly blunted by treatment with the FAO inhibitor etomoxir (Fig. 3 *N* and *O*), thus suggesting that elevated VCP in CRC promotes cell growth by upregulating FAO.

VCP Inhibition Represses FAO in CRC. VCP is recognized as an attractive target for cancer drug development (35). VCP Inhibition leads to proteotoxic stress and cell death. However, researchers have also mentioned that the induction of cancer cell death upon VCP inhibition includes additional mechanisms (17). Therefore,

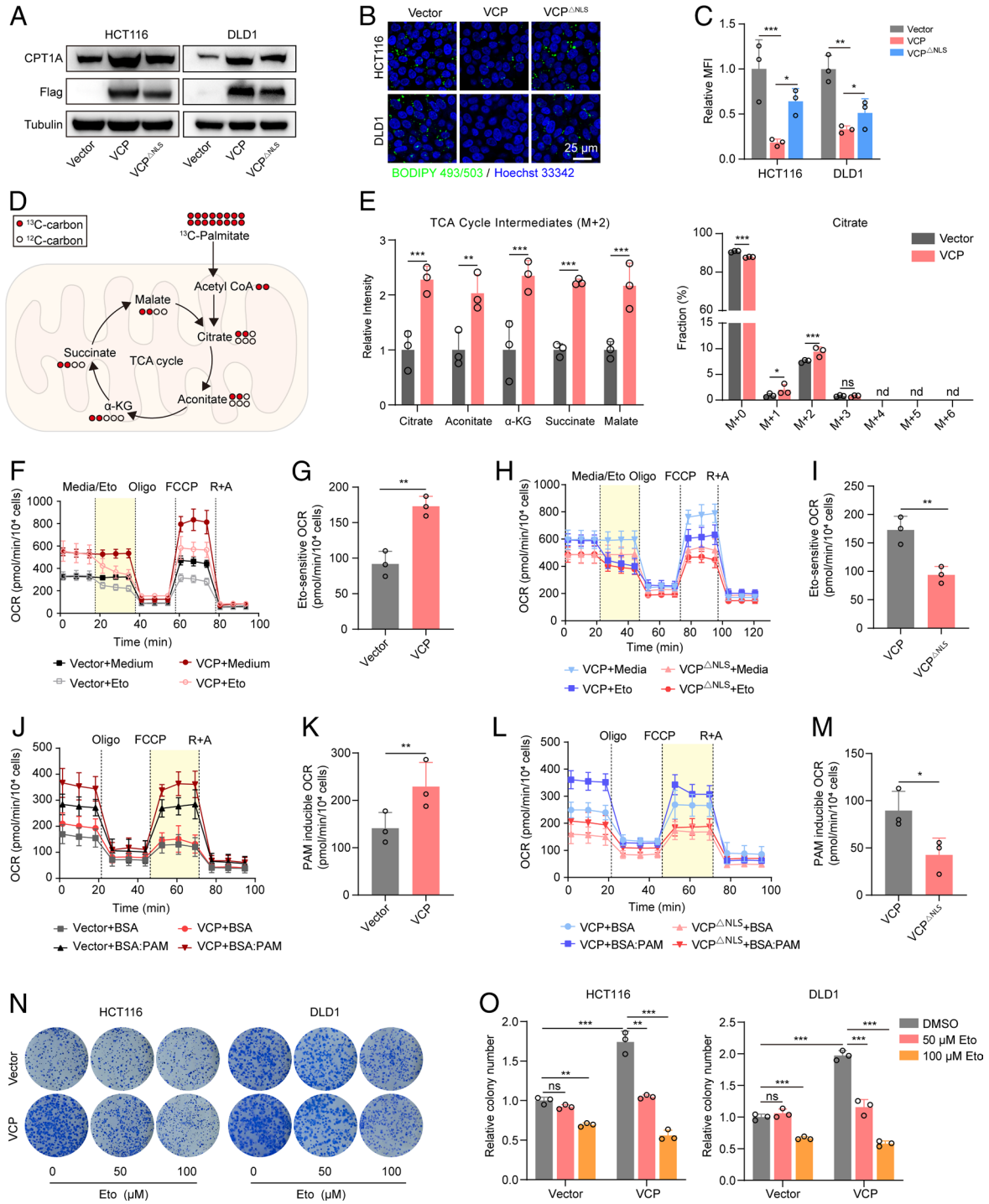

Fig. 3. Nuclear VCP promotes FAO in CRC. (*A*) Western blot analysis of CPT1A and Flag-VCP in cells stably expressing Flag-tagged VCP, VCP$^{\triangle NLS,}$ or control vector. (*B* and *C*) BIODIPY 493/503 staining was used to determine the content of lipid droplets in cells stably expressing VCP, VCP$^{\triangle NLS}$, or control vector (Scale bar, 25 μm). (*C*) The mean fluorescence intensity (MFI) was quantified, $n = 3$. (*D* and *E*) Metabolic tracing analysis of ^{13}C-labeled palmitate in HCT116 cells stably expressing VCP or control vector. (*E*) The relative intensity of M + 2 citrate and other indicated TCA metabolites (*Left*), as well as the fraction of each isotopomer for the citrate pool (*Right*), is shown, $n = 3$. (*F–I*) OCR were measured at baseline and in response to media, etomoxir (Eto), oligomycin (Oligo), FCCP, and rotenone plus antimycin A (R + A) in vector-/VCP-expressed HCT116 cells (*F* and *G*) and VCP-/VCP$^{\triangle NLS}$-expressed HCT116 cells (*H* and *I*). Eto-sensitive OCR (yellow areas) was quantified. Eto-sensitive OCR = OCR (Medium) -OCR (Eto), $n = 3$. (*J–M*) OCR of HCT116 cells, stably expressing vector or VCP (*J* and *K*) and stably expressing VCP or VCP$^{\triangle NLS}$ (*L* and *M*) in response to palmitate (PAM)-containing medium. PAM-induced OCR (yellow areas) was quantified. PAM-induced OCR = OCR (BSA:PAM) − OCR (BSA), $n = 3$. (*N* and *O*) Colony formation assay of HCT116 and DLD1 cells stably expressing VCP or control vector after treatment with the indicated concentrations of etomoxir (Eto). (*O*) Colony number was quantified, $n = 3$. Data for (*F*), (*H*), (*J*), and (*L*) represent one of three independent experiments each contain three replicates. Data represent the mean ± SD. ns: not significant, nd: not detected, $^{*}P < 0.05$; $^{**}P < 0.01$; $^{***}P < 0.001$. *P* values were determined by Student's *t* test for (*E*, *G*, *I*, *K* and *M*), one-way ANOVA for (*C*) or two-way ANOVA for (*O*). See also *SI Appendix*, Fig. S4.

we investigated whether FAO participates in the tumor cell death induced by VCP inhibition. Our data revealed that as expected, knockdown of VCP significantly hindered CRC cell growth (*SI Appendix*, Fig. S5). Furthermore, CPT1A protein expression was significantly decreased upon VCP knockdown (Fig. 4*A*). We observed that knockdown of VCP induced the accumulation of adiposomes in CRC cells, thus suggesting that fatty acid utilization was reduced (*SI Appendix*, Fig. S6 *A* and *B*). Additionally, ATP

and NADPH production was decreased in VCP-knockdown cells (*SI Appendix*, Fig. S6 *C* and *D*). Furthermore, knockdown of VCP caused an overall reduction in TCA cycle intermediates from ^{13}C-palmitate in CRC cells (Fig. 4*B* and *SI Appendix*, Fig. S6*E*). Finally, the levels of both Eto-sensitive OCR and PAM-induced OCR in the VCP-knockdown cells were significantly lower than those in control cells (Fig. 4 *C*–*F* and *SI Appendix*, Fig. S6 *F* and *G*). These data suggested that VCP inhibition represses FAO in CRC cells.

To test whether the decreased FAO is involved in CRC cell death caused by VCP inhibition, we supplied myristic acid (medium chain fatty acid) and the FAO agonist bezafibrate to the VCP-knockdown cells. Our data showed that both treatments rescued the inhibited clonogenic capacity caused by VCP knockdown to varying degrees (*SI Appendix*, Fig. S6 *H* and *I*). Moreover, acetate supplementation, which replenishes acetyl-CoA levels, also rescued the inhibited clonogenic capacity caused by VCP knockdown (*SI Appendix*, Fig. S6 *J* and *K*). Taken together, our results revealed that repressed FAO plays an important role in CRC cell death induced by VCP inhibition.

Nuclear VCP Regulates the Transcription of CPT1A via HDAC1. Recent findings have revealed the roles of VCP in fundamental chromatin-associated processes that ensure proper transcription (12). For example, VCP has been demonstrated in yeast to remove the ubiquitinated transcription repressor α2 complex from promoter elements during mating-type transition (36). We thus hypothesized that VCP might regulate the transcription of FAO genes by mediating chromatin-associated protein degradation. First, we confirmed that VCP was enriched and bound to chromatin in CRC cells (Fig. 5 *A* and *B*). Second, chromatin immunoprecipitation coupled with sequencing (ChIP-seq) and ChIP-quantitative PCR (ChIP-qPCR) analyses suggested that the key FAO gene *CPT1A* harbors VCP-binding elements in its promoter with enhanced binding upon VCP-overexpression (Fig. 5 *C* and *D and SI Appendix*, Fig. S7 *A*–*D*). Third, cloning of the CPT1A fragments in the luciferase reporter showed that overexpression of VCP enhanced the luciferase activity (Fig. 5*E*). Conversely, VCP knockdown attenuated the luciferase activity of *CPT1A* (Fig. 5*F*). These results indicated that VCP binds to chromatin and positively regulates the transcription of the key FAO gene *CPT1A*.

To identify the underlying mechanism of transcriptional regulation of *CPT1A* by VCP, we immunoprecipitated exogenous flag-tagged VCP from CRC cells and identified the interacting proteins using mass spectrometry. In addition to UFD1 and NPL4 (the well-known cofactors of VCP), HDAC1 was identified as an interacting protein of VCP in CRC cells (*SI Appendix*, Fig. S7 *E* and *F*). Further, we performed coimmunoprecipitation and a Duolink PLA to determine whether VCP interacts with HDAC1 in the nucleus. Our data indicated that the binding between VCP and HDAC1 occurred in the nucleus (Fig. 5 *G* and *H* and *SI Appendix*, Fig. S7*G*). HDACs are components of large transcriptional corepressor complexes, which are recruited by transcription factors to specific promoter regions to mediate transcriptional repression. Our data revealed that treatment with a HDAC1/2

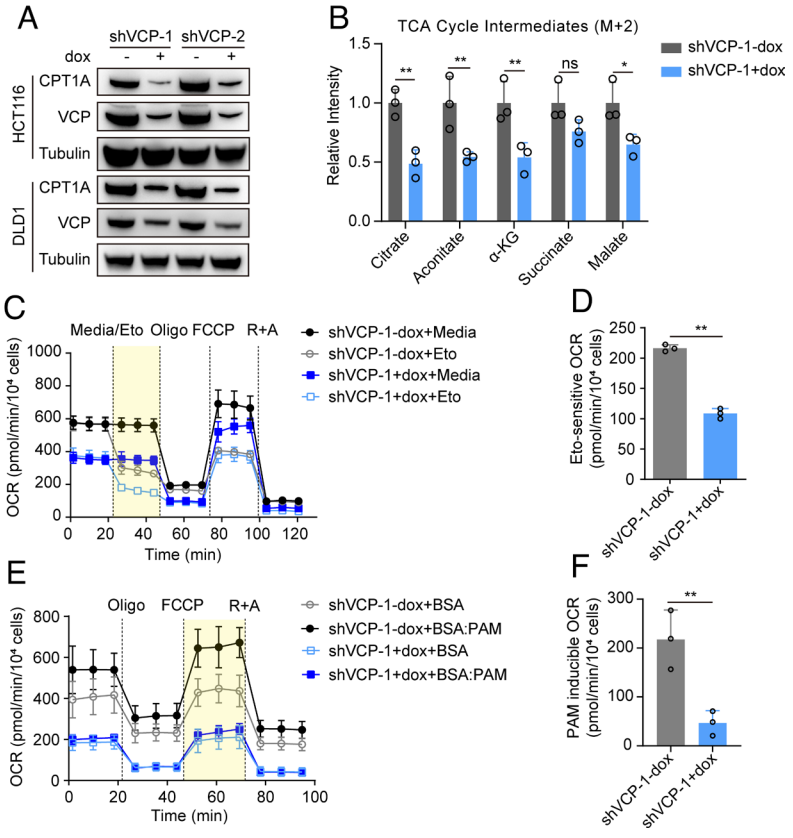

Fig. 4. VCP inhibition attenuates FAO in CRC. (*A*) Western blot analysis of CPT1A and VCP in cells transfected with dox-inducible shVCP in the absence or presence of dox. (*B*) Metabolic tracing analysis of ^{13}C-labeled palmitate in HCT116 cells transfected with dox-inducible shVCP in the absence or presence of dox. The relative intensity of M + 2 citrate and other indicated TCA metabolites is shown, $n = 3$. (*C*) OCR values of cells transfected with shVCP in the presence or absence of dox were measured at baseline and in response to media, etomoxir (Eto), oligomycin (Oligo), FCCP, and rotenone plus antimycin A (R + A). (*D*) Eto-sensitive OCR (yellow areas) was quantified, $n = 3$. (*E*) OCR values of cells transfected with shVCP in the presence or absence of dox in response to palmitate (PAM)-containing medium. (*F*) PAM-induced OCR (yellow areas) was quantified, $n = 3$. Data for (*C*) and (*E*) represent one of three independent experiments each contain three replicates. Data represent the mean ± SD. ns: not significant, $^{*}P < 0.05$, $^{**}P < 0.01$, $^{***}P < 0.001$. *P* values were determined by Student's *t* test. See also *SI Appendix*, Figs. S5 and S6.

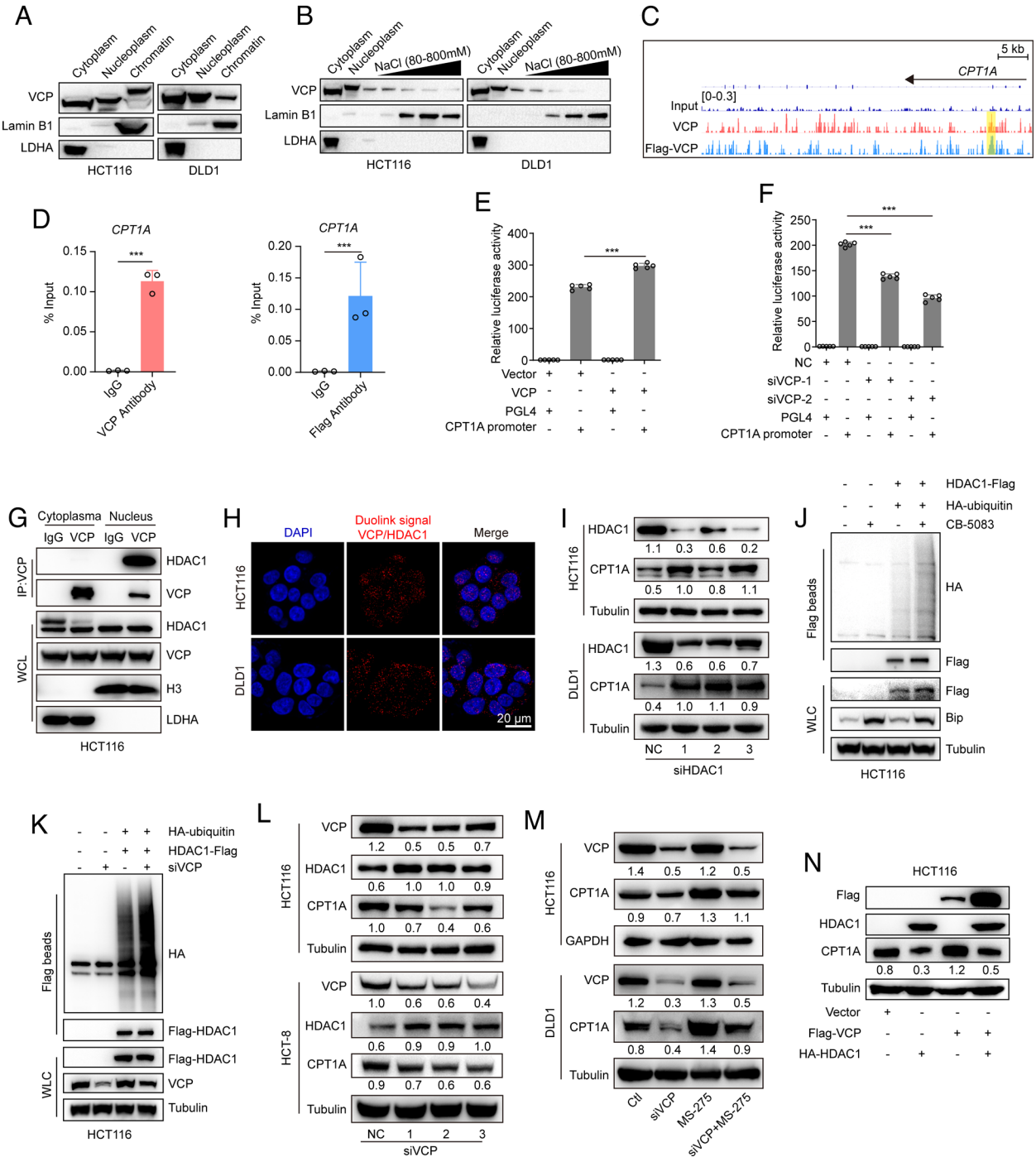

Fig. 5. Nuclear VCP promotes CPT1A transcription in a HDAC1-dependent manner. (*A*) Western blot analysis of VCP in the cytoplasmic, nucleoplasmic, and chromatin fractions of the indicated cells. (*B*) The chromatin fractions of the indicated cells were extracted with increasing concentrations of NaCl (80–800 mM) and western blots were then performed to determine the distribution of VCP. (*C*) Representative ChIP-seq signal (*CPT1A* locus) for VCP in HCT116 cells stably expressing VCP or Flag-tagged VCP. The yellow area represents the binding site of VCP in the promoter of *CPT1A*. (*D*) ChIP-qPCR analysis of VCP binding to the *CPT1A* promoter in HCT116 cells stably expressing VCP or Flag-tagged VCP. DNA enrichment was calculated as percentage of input, with normal IgG as control, $n = 3$. (*E*) *CPT1A* promoter-Luciferase assay was measured in HCT116 cells after cotransfection with the indicated plasmids, $n = 5$. (*F*) *CPT1A* promoter-Luciferase assay was measured in HCT116 cells after cotransfection with VCP siRNAs and the indicated plasmids, $n = 5$. (*G*) Cytoplasmic or nuclear extracts from HCT116 cells treated with MG-132 were collected for IP with either nonspecific IgG or with an antibody against VCP and immunoblotted as indicated. WCL, whole cell lysates. (*H*) Detection of endogenous VCP and HDAC1 binding (red dots) was performed by Duolink proximity ligation assay (PLA) assay (Scale bar, 20 μm). (*I*) Western blot analysis of indicated proteins in cells transfected with control (NC) or HDAC1 siRNAs. (*J* and *K*) Immunoblot of WCL and Flag beads pull-down products derived from HCT116 cells treated with CB-5083 (0.3 μM, 24 h) or transfected with VCP siRNA and cotransfected with the indicated plasmids. (*L*) Western blot analysis of the indicated proteins in cells transfected with control (NC) or VCP siRNAs. (*M*) Western blot analysis of the indicated proteins in cells treated with siRNA targeting VCP (siVCP), MS-275 (2 μM), or siVCP/MS-275 for 24 h. (*N*) Western blot analysis of the indicated proteins in cells transfected with the indicated plasmids. Data represent mean ± SD. $^{***}P < 0.001$. *P* values were determined by Student's *t* test for (*D*) or one-way ANOVA for (*E* and *F*). See also *SI Appendix*, Fig. S7.

inhibitor (MS-275) or siRNAs target HDAC1 significantly increased the expression of CPT1A in CRC cells (Fig. 5*I* and *SI Appendix*, Fig. S7*H*).

We next investigated whether VCP could extract ubiquitinated HDAC1 from chromatin and promote its degradation. Our results revealed that the levels of ubiquitinated HDAC1 were significantly

increased in CRC cells that were treated with a VCP inhibitor (CB-5083) or with siRNA against VCP (Fig. 5 *J* and *K*). Furthermore, in agreement with our hypothesis, VCP knockdown resulted in increased HDAC1 protein expression and reduced CPT1A protein expression (Fig. 5*L*). Next, we assessed the dependence of VCP-modulated FAO on the HDAC1 regulatory axis. Our data demonstrated that knockdown of VCP suppressed the expression of CPT1A, while the HDAC1/2 inhibitor MS-275 reversed the decrease in CPT1A protein level induced by siVCP (Fig. 5*M*). Furthermore, VCP overexpression did not up-regulate CPT1A expression in the presence of exogenous HDAC1 (Fig. 5*N*). Taken together, our results identify a unique VCP–HDAC1–FAO pathway that is critical for CRC growth.

VCPI Cooperates with Metformin to Impair CRC Cell Growth by Suppressing FAO. A recent study suggested that FAO is activated in response to metformin treatment to fuel the TCA cycle in environments with limited glucose availability, and this may hinder the anticancer effects of metformin (27). Considering that VCP inhibition can repress FAO, we next investigated the effects of VCP inhibitor (VCPI)/metformin combination therapy. We chose a potent and selective VCP inhibitor (CB-5083) that is currently being evaluated in two clinical trials in patients with relapsed and refractory multiple myeloma and in patients with advanced solid tumors (18). As CB-5083 targets the ATPase activity of VCP, we first determined whether ATPase activity could affect the transport of VCP into the nucleus. We generated a catalytic D1 or D2 ATPase domain mutant of VCP by replacing a lysine residue at position 251 or 524 with alanine (VCP^{K251A} and VCP^{K524A}) as previously described (37). As the data showed, both VCP^{K251A} and VCP^{K524A} hindered the transport of VCP into the nuclei of CRC cells (*SI Appendix*, Fig. S8*A*). Thus, it is unsurprising that CB-5083 that possesses a D2 ATPase selectivity of VCP was able to block the entry of VCP into the nucleus, thereby inhibiting CRC cell growth (*SI Appendix*, Fig. S8 *B* and *C*). Further investigation demonstrated that CB-5083 down-regulated the protein level of CPT1A and induced the accumulation of adiposomes (Fig. 6 *A*–*C*), thus suggesting that CB-5083 was able to repress FAO in CRC cells.

Metformin can activate AMP-activated protein kinase (AMPK) and inhibit the synthesis of long-chain fatty acids by inhibiting acetyl-CoA carboxylase (ACC), thus promoting FAO of long-chain fatty acids by enabling the import of fatty acyl-CoA molecules into mitochondria (38, 39). Our data also confirmed that metformin treatment resulted in higher PAM-stimulated OCR compared to that observed with the vehicle group, thus indicating that FAO is activated after metformin treatment in CRC cells (Fig. 6 *D* and *E*). However, we observed that the VCP inhibitor CB-5083 appeared to inhibit metformin-mediated upregulation of FAO capacity as indicated by the decreased PAM-stimulated OCR (Fig. 6 *D* and *E*). Immunoblotting analysis further demonstrated that CB-5083 blocked metformin-induced upregulation of CPT1A levels (Fig. 6*F*). Finally, the combination of CB-5083 and metformin resulted in a significantly stronger inhibition of CRC cell growth than did individual treatments (Fig. 6*G*), and similar results were obtained in cells under glucose deprivation in the presence of palmitate acid (Fig. 6*H*).

Combination Treatment with VCP Inhibitor and Metformin Effectively Inhibits Tumor Growth in CRC Tumors. Based on the synergy between VCPI and metformin in CRC cells, we first evaluated the therapeutic potential of VCPI/metformin combination therapy in established HCT116 xenografts. In agreement with the in vitro observations, the combined treatment resulted in significantly stronger inhibition of tumor growth in HCT116 xenografts compared with single agents (Fig. 7*A* and *SI Appendix*, Fig. S9*A*). Additionally, luminescent imaging analysis of tumor-bearing mice further validated the enhanced antitumor effects of the combination therapy (Fig. 7*B* and *SI Appendix*, Fig. S9 *B* and *C*). Next, we investigated the antitumor efficacy of VCPI/metformin combination therapy in two PDX. Consistent with earlier results, CB-5083 or metformin alone exerted minimal effects on tumor growth, while combination therapy markedly reduced the tumor burden in the two PDX models (Fig. 7*C* and *SI Appendix*, Fig. S9 *D* and *E*).

Furthermore, IHC analysis of tumor tissues revealed a significant decrease in cell proliferation in the combined treatment group compared to that observed with the single treatments (Fig. 7*D* and *SI Appendix*, Fig. S9*F*). In agreement with our in vitro results, both IHC and immunoblotting analyses demonstrated that VCPI CB-5083 notably abrogated the upregulation of CPT1A induced by metformin (Fig. 7*D* and *SI Appendix*, Fig. S9 *F* and *G*). Together, these data support our concept of combination therapy incorporating VCP inhibitor and metformin for the effective treatment of CRC.

Discussion

Metabolic reprogramming is one of the hallmarks of cancer (40). Numerous studies have provided mechanistic insights into why tumors up-regulate glucose uptake and metabolism (41). However, our understanding of tumor metabolism is incomplete, as numerous tumors are FDG-PET negative (42). This suggests that many cancers utilize alternate carbon sources. Increasing data suggest that highly proliferative cancer cells exhibit strong lipid avidity that they satisfy by either increasing lipid uptake from exogenous sources or by over-activating their endogenous synthesis (43). Fatty acids have been demonstrated to be required for energy storage, membrane formation, and the generation of signaling molecules within solid tumors to overcome harsh environments, and alterations in fatty acid metabolism in cancer cells have received increasing attention (44). With most cancer researchers focusing on fatty acid synthesis (FAS), the relevance of FAO for cancer cell function has not been carefully explored (8), particularly in certain types of cancers that are close to adipose tissue.

FAO is a multistep catabolic process that allows for the mitochondrial conversion of long-chain fatty acids into acetyl-CoA that then participates in the Krebs' cycle to generate NADPH, NADH, FADH2, and ATP (33, 45). Fatty acids provide much more ATP than do carbohydrates when completely oxidized in mitochondria, and therefore, FAO is important for tumor cells in regard to overcoming metabolic stress under conditions involving nutrient limitation. FAO is an important source of cytosolic NADPH for cancer cells to maintain redox homeostasis and cell survival, particularly under glucose deprivation (8). Substantial studies have revealed the overexpression of various FAO enzymes, including CPT1, carnitine transporter CT2, and acyl-CoA synthetase long-chain 3 in multiple malignancies (46–49). Therefore, key enzymes and regulators of FAO have emerged as promising targets for cancer therapy. For example, genetic or pharmacological loss-of-function approaches have revealed that targeting CPT1 is an effective approach for inhibiting tumor growth in adipose environments (50).

Currently, how VCP contributes to CRC progression remains poorly understood. VCP is best known for its role in ubiquitin-dependent proteasomal degradation of aberrant endoplasmic reticulum (ER) proteins (51). However, our study suggests that exogenously expressed VCP can promote CRC growth in an ERAD-deficient model, thus indicating that other functions of VCP are

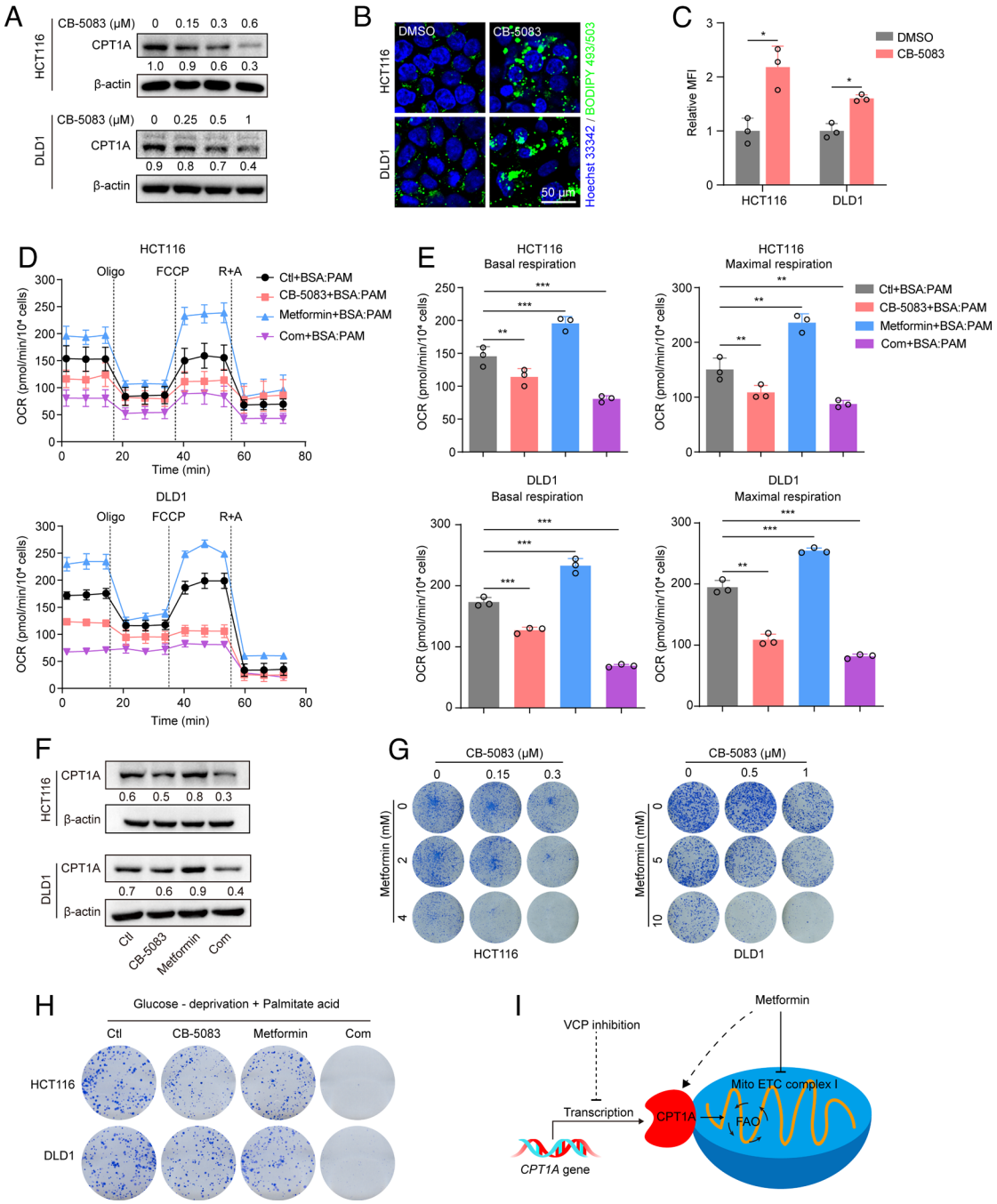

Fig. 6. VCPI cooperates with metformin to impair CRC cell growth by suppressing FAO. (*A*) Western blot analysis of CPT1A in cells treated with increasing concentrations of CB-5083 for 24 h. (*B* and *C*) BIODIPY 493/503 staining was used to determine the content of lipid droplet in cells treated with CB-5083 (HCT116, 0.3 μM; DLD1, 1 μM) for 24 h. (*C*) The MFI was quantified (Scale bar, 50 μm), $n = 3$. (*D* and *E*) Cells were treated with CB-5083 (HCT116, 0.3 μM; DLD1, 1 μM), metformin (HCT116, 10 mM; DLD1, 20 mM), or a combination, and this was followed by OCR measurement in response to palmitate (PAM)-containing medium. (*E*) Basal and maximal respiration was quantified, $n = 3$. (*F*) Western blot analysis of CPT1A in cells treated with CB-5083 (HCT116, 0.3 μM; DLD1, 1 μM), metformin (HCT116, 10 mM; DLD1, 20 mM), or a combination for 24 h. The levels of CPT1A were quantified. (*G*) Colony formation assay of cells treated with CB-5083, metformin or a combination at the indicated concentrations. (*H*) Cells were cultured in DMEM with low glucose (2.5 mM glucose) and palmitate acid (25 μM), colony formation assay was performed after treatment with CB-5083 (HCT116, 0.15 μM; DLD1, 0.5 μM), metformin (HCT116, 2 mM; DLD1, 5 mM) or a combination. (*I*) Graphical model of VCP inhibitor and metformin combination therapy. Data for (*D*) represent one of three independent experiments each contain three replicates. Data represent mean ± SD. $^{*}P < 0.05$, $^{**}P < 0.01$, $^{***}P < 0.001$. *P* values were determined by Student's *t* test for (*C*), or one-way ANOVA for (*E*). See also *SI Appendix*, Fig. S8.

involved in driving CRC progression. By deleting the NLS of VCP, we discovered that nuclear VCP is critical for CRC progression. Thus, we describe a noncanonical mechanism of VCP in promoting CRC growth. Furthermore, we provide evidence that nuclear VCP specifically binds to HDAC1 and that chemical inhibition or knockdown of VCP results in increased HDAC1 ubiquitylation and increased HDAC1 protein levels, thus suppressing FAO gene transcription. Collectively, these results suggest that a unique VCP–HDAC1–FAO pathway drives CRC progression. Further investigation of the molecular interactions between VCP and HDAC1 in the nucleus may yield important information.

Mitochondrial metabolism has emerged as an attractive target for cancer therapy (52, 53). In particular, the antidiabetic drug metformin has been reported to inhibit mitochondrial ETC complex I

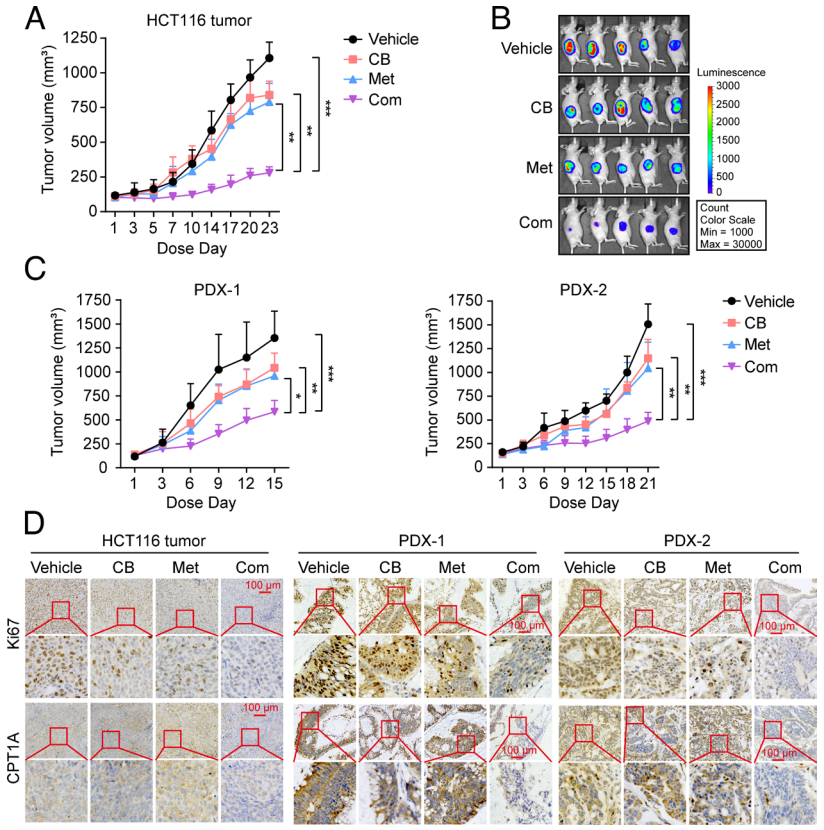

Fig. 7. Combination treatment with VCP inhibitor and metformin effectively inhibits tumor growth in CRC tumors. (*A*) Luciferase-labeled HCT116 xenografts were treated with vehicle, CB-5083 (30 mg/kg), metformin (200 mg/kg), or a combination, $n = 5$ mice per group. (*B*) In vivo tumor bioluminescence images of mice from (*A*) at the end of the experiment. (*C*) PDX mice were treated with vehicle, CB-5083 (40 mg/kg), metformin (200 mg/kg), or a combination, $n = 5$ mice per group. (*D*) Immunohistochemistry (IHC) analysis of Ki67 (a marker of proliferation) and CPT1A (a marker of the FAO pathway) in tumor tissues from (*A* and *C*) (Scale bar, 100 μm). CB: CB-5083, Met: metformin, Com: Combination. Data represent mean ± SD. $^{*}P < 0.05$, $^{**}P < 0.01$, $^{***}P < 0.001$. Tumor volume values were analyzed using repeated-measures one-way ANOVA. See also *SI Appendix*, Fig. S9.

and reduce tumor growth (54, 55). Due to strong retrospective clinical evidence and laboratory-based studies, there are more than 100 ongoing clinical trials assessing the anticancer effects of metformin in combination with current standard treatments (56). Treatment with metformin has been reported to inhibit mitochondrial complex I activity in cancer cells (54) and lead to metabolic stress and FAO activation (27, 39). In this study, we found that metformin significantly increased FAO activity and CPT1A expression in CRC, and this could be blocked by the use of VCP inhibitor (Fig. 6*I*). Based on this, our data demonstrated that the combination of VCP inhibitor and metformin produced superior anticancer effects compared with monotherapies. Taken together, our findings created a combination therapy consisting of VCP inhibitors and metformin that would be particularly effective for the treatment of CRCs.

Overall, our study offers insights into mechanisms that drive fatty acid oxidation in tumors and provides a rationale for clinical studies directed at exploring VCP inhibitors in combination with metformin for the treatment of CRC.

Materials and Methods

This research complies with all relevant ethical regulations. All of the mouse experiments described in this study were approved by the Laboratory Animal Ethics Committee of Jinan University. All of the cell lines were generously gifted by Mong-Hong Lee (The Sixth Affiliated Hospital of Sun Yat-sen University, Guangzhou, China). Details of materials and methods are described in *SI Appendix*, *Materials and Methods*.

Data, Materials, and Software Availability. All the sequencing data in this paper have been deposited in GEO database, https://www.ncbi.nlm.nih.gov/geo/. RNA sequencing and ChIP sequencing data are accessible through GEO series accession numbers GSE201660 (57) and GSE201200 (58), respectively. They are publicly available. All other study data are included in the article and *SI Appendix*.

ACKNOWLEDGMENTS. We thank Prof. Mong-Hong Lee (The Sixth Affiliated Hospital of Sun Yat-sen University) for the technical support. This work was supported by grants from the National Natural Science Foundation of China (81972605 to H.Z. 82173829 to F.X.), the Guangdong Natural Science Funds of Distinguished Young Scholar (2021B1515020067 to H.Z.), and the Pearl River S&T Nova Program of Guangzhou (201906010069 to H.Z.).

Author affiliations: [a]Department of Pharmacology, School of Medicine, Jinan University, Guangzhou 510632, China; [b]Guangdong Provincial Key Laboratory of Tumor Interventional Diagnosis and Treatment, Zhuhai Institute of Translational Medicine, Zhuhai People's Hospital Affiliated with Jinan University, Zhuhai 519000, China; [c]Biomedical Translational Research Institute, Health Science Center (School of Medicine), Jinan University, Guangzhou 510632, China; [d]Department of Public Health, Shantou Center for Disease Control and Prevention, Shantou 515000, China; [e]Guangdong Research Institute of Gastroenterology, The Sixth Affiliated Hospital of Sun Yat-sen University, Guangzhou 510655, China; [f]Department of Pathophysiology, School of Basic Medical Sciences, Peking University, Beijing 100191, China; and [g]Medical Research Institute, Guangdong Provincial People's Hospital (Guangdong Academy of Medical Sciences), Southern Medical University, Guangzhou 510080, China

1. N. J. German *et al.*, PHD3 loss in cancer enables metabolic reliance on fatty acid oxidation via deactivation of ACC2. *Mol. Cell* **63**, 1006–1020 (2016).
2. B. Lauby-Secretan *et al.*, Body fatness and cancer–Viewpoint of the IARC Working Group. *N. Engl. J. Med.* **375**, 794–798 (2016).
3. J. C. Brown *et al.*, The association of abdominal adiposity with mortality in patients with stage I-III colorectal cancer. *J. Natl. Cancer Inst.* **112**, 377–383 (2020).
4. Y. A. Wen *et al.*, Adipocytes activate mitochondrial fatty acid oxidation and autophagy to promote tumor growth in colon cancer. *Cell Death Dis.* **8**, e2593 (2017).

5. Y. Y. Wang *et al.*, Mammary adipocytes stimulate breast cancer invasion through metabolic remodeling of tumor cells. *JCI Insight* **2**, e87489 (2017).
6. I. Lazar *et al.*, Adipocyte exosomes promote melanoma aggressiveness through fatty acid oxidation: A novel mechanism linking obesity and cancer. *Cancer Res.* **76**, 4051–4057 (2016).
7. R. A. Cairns, I. S. Harris, T. W. Mak, Regulation of cancer cell metabolism. *Nat. Rev. Cancer* **11**, 85–95 (2011).
8. A. Carracedo, L. C. Cantley, P. P. Pandolfi, Cancer metabolism: Fatty acid oxidation in the limelight. *Nat. Rev. Cancer* **13**, 227–232 (2013).
9. T. Wang *et al.*, JAK/STAT3-regulated fatty acid beta-oxidation is critical for breast cancer stem cell self-renewal and chemoresistance. *Cell Metab.* **27**, 136–150.e135 (2018).
10. Y. N. Wang *et al.*, CPT1A-mediated fatty acid oxidation promotes colorectal cancer cell metastasis by inhibiting anoikis. *Oncogene* **37**, 6025–6040 (2018).
11. X. X. Li *et al.*, Nuclear receptor Nur77 facilitates melanoma cell survival under metabolic stress by protecting fatty acid oxidation. *Mol. Cell* **69**, 480–492.e487 (2018).
12. H. Meyer, M. Bug, S. Bremer, Emerging functions of the VCP/p97 AAA-ATPase in the ubiquitin system. *Nat. Cell Biol.* **14**, 117–123 (2012).
13. N. P. Dantuma, T. Hoppe, Growing sphere of influence: Cdc48/p97 orchestrates ubiquitin-dependent extraction from chromatin. *Trends Cell Biol.* **22**, 483–491 (2012).
14. S. Yamamoto *et al.*, Expression of valosin-containing protein in colorectal carcinomas as a predictor for disease recurrence and prognosis. *Clin. Cancer Res.* **10**, 651–657 (2004).
15. S. Yamamoto *et al.*, Expression level of valosin-containing protein is strongly associated with progression and prognosis of gastric carcinoma. *J. Clin. Oncol.* **21**, 2537–2544 (2003).
16. S. Yamamoto *et al.*, Elevated expression of valosin-containing protein (p97) in hepatocellular carcinoma is correlated with increased incidence of tumor recurrence. *J. Clin. Oncol.* **21**, 447–452 (2003).
17. P. Magnaghi *et al.*, Covalent and allosteric inhibitors of the ATPase VCP/p97 induce cancer cell death. *Nat. Chem. Biol.* **9**, 548–556 (2013).
18. D. J. Anderson *et al.*, Targeting the AAA ATPase p97 as an approach to treat cancer through disruption of protein homeostasis. *Cancer Cell* **28**, 653–665 (2015).
19. H. P. Zhang *et al.*, Targeting VCP enhances anticancer activity of oncolytic virus M1 in hepatocellular carcinoma. *Sci. Transl. Med.* **9**, eaam7996 (2017).
20. R. Le Moigne *et al.*, The p97 inhibitor CB-5083 is a unique disrupter of protein homeostasis in models of multiple myeloma. *Mol. Cancer Ther.* **16**, 2375–2386 (2017).
21. J. B. Heidelberger *et al.*, Proteomic profiling of VCP substrates links VCP to K6-linked ubiquitylation and c-Myc function. *EMBO Rep.* **19**, e44754 (2018).
22. D. B. Krastev *et al.*, The ubiquitin-dependent ATPase p97 removes cytotoxic trapped PARP1 from chromatin. *Nat. Cell Biol.* **24**, 62–73 (2022).
23. T. V. Nguyen *et al.*, p97/VCP promotes degradation of CRBN substrate glutamine synthetase and neosubstrates. *Proc. Natl. Acad. Sci. U.S.A.* **114**, 3565–3571 (2017).
24. G. J. van der Windt *et al.*, Mitochondrial respiratory capacity is a critical regulator of CD8+ T cell memory development. *Immunity* **36**, 68–78 (2012).
25. M. D. Fullerton *et al.*, Single phosphorylation sites in Acc1 and Acc2 regulate lipid homeostasis and the insulin-sensitizing effects of metformin. *Nat. Med.* **19**, 1649–1654 (2013).
26. Y. Wang *et al.*, Metformin improves mitochondrial respiratory activity through activation of AMPK. *Cell Rep.* **29**, 1511–1523.e1515 (2019).
27. X. Liu, I. L. Romero, L. M. Litchfield, E. Lengyel, J. W. Locasale, Metformin targets central carbon metabolism and reveals mitochondrial requirements in human cancers. *Cell Metab.* **24**, 728–739 (2016).
28. Z. Zhou *et al.*, Endoplasmic reticulum-associated degradation regulates mitochondrial dynamics in brown adipocytes. *Science* **368**, 54–60 (2020).
29. S. Sun *et al.*, IRE1α is an endogenous substrate of endoplasmic-reticulum-associated degradation. *Nat. Cell Biol.* **17**, 1546–1555 (2015).
30. X. Shi, K. Zhu, Z. Ye, J. Yue, VCP/p97 targets the nuclear export and degradation of p27(Kip1) during G1 to S phase transition. *FASEB J.* **34**, 5193–5207 (2020).
31. J. Xiong, Fatty acid oxidation in cell fate determination. *Trends Biochem. Sci.* **43**, 854–857 (2018).
32. I. R. Schlaepfer, M. Joshi, CPT1A-mediated fat oxidation, mechanisms, and therapeutic potential. *Endocrinology* **161**, bqz046 (2020).
33. A. Carracedo, L. C. Cantley, P. P. Pandolfi, Cancer metabolism: fatty acid oxidation in the limelight. *Nat. Rev. Cancer* **13**, 227–232 (2013).
34. R. J. Deberardinis, J. J. Lum, C. B. Thompson, Phosphatidylinositol 3-kinase-dependent modulation of carnitine palmitoyltransferase 1A expression regulates lipid metabolism during hematopoietic cell growth. *J. Biol. Chem.* **281**, 37372–37380 (2006).
35. S. Banerjee *et al.*, 2.3 angstrom resolution cryo-EM structure of human p97 and mechanism of allosteric inhibition. *Science* **351**, 871–875 (2016).
36. A. J. Wilcox, J. D. Laney, A ubiquitin-selective AAA-ATPase mediates transcriptional switching by remodelling a repressor-promoter DNA complex. *Nat. Cell Biol.* **11**, 1481–1486 (2009).
37. C. Song *et al.*, Nucleocytoplasmic shuttling of valosin-containing protein (VCP/p97) regulated by its N domain and C-terminal region. *Biochim. Biophys. Acta* **1853**, 222–232 (2015).
38. L. He, Metformin and systemic metabolism. *Trends Pharmacol. Sci.* **41**, 868–881 (2020).
39. M. Foretz, B. Guigas, L. Bertrand, M. Pollak, B. Viollet, Metformin: From mechanisms of action to therapies. *Cell Metab.* **20**, 953–966 (2014).
40. D. Hanahan, R. A. Weinberg, Hallmarks of cancer: The next generation. *Cell* **144**, 646–674 (2011).
41. S. Y. Lunt, M. G. Vander Heiden, Aerobic glycolysis: Meeting the metabolic requirements of cell proliferation. *Annu. Rev. Cell Dev. Biol.* **27**, 441–464 (2011).
42. N. M. Long, C. S. Smith, Causes and imaging features of false positives and false negatives on F-PET/CT in oncologic imaging. *Insights Imaging* **2**, 679–698 (2011).
43. S. Beloribi-Djefaflia, S. Vasseur, F. Guillaumond, Lipid metabolic reprogramming in cancer cells. *Oncogenesis* **5**, e189 (2016).
44. E. Currie, A. Schulze, R. Zechner, T. C. Walther, R. V. Farese Jr., Cellular fatty acid metabolism and cancer. *Cell Metab.* **18**, 153–161 (2013).
45. Y. B. Ma *et al.*, Fatty acid oxidation: An emerging facet of metabolic transformation in cancer. *Cancer Lett.* **435**, 92–100 (2018).
46. E. Currie, A. Schulze, R. Zechner, T. C. Walther, R. V. Farese, Cellular fatty acid metabolism and cancer. *Cell Metab.* **18**, 153–161 (2013).
47. G. Pascual *et al.*, Targeting metastasis-initiating cells through the fatty acid receptor CD36. *Nature* **541**, 41–45 (2017).
48. M. S. Padanad *et al.*, Fatty acid oxidation mediated by Acyl-CoA synthetase long chain 3 is required for mutant KRAS lung tumorigenesis. *Cell Rep.* **16**, 1614–1628 (2016).
49. T. Y. Wang *et al.*, JAK/STAT3-regulated fatty acid beta-oxidation is critical for breast cancer stem cell self-renewal and chemoresistance. *Cell Metab.* **27**, 136–150.e5 (2018).
50. H. Iwamoto *et al.*, Cancer lipid metabolism confers antiangiogenic drug resistance. *Cell Metab.* **28**, 104–117.e105 (2018).
51. D. Fessart, E. Marza, S. Taouji, F. Delom, E. Chevet, P97/CDC-48: Proteostasis control in tumor cell biology. *Cancer Lett.* **337**, 26–34 (2013).
52. M. G. Vander Heiden, R. J. DeBerardinis, Understanding the intersections between metabolism and cancer biology. *Cell* **168**, 657–669 (2017).
53. S. E. Weinberg, N. S. Chandel, Targeting mitochondria metabolism for cancer therapy. *Nat. Chem. Biol.* **11**, 9–15 (2015).
54. W. W. Wheaton *et al.*, Metformin inhibits mitochondrial complex I of cancer cells to reduce tumorigenesis. *eLife* **3**, e02242 (2014).
55. X. J. Liu, I. L. Romero, L. M. Litchfield, E. Lengyel, J. W. Locasale, Metformin targets central carbon metabolism and reveals mitochondrial requirements in human cancers. *Cell Metab.* **24**, 728–739 (2016).
56. M. Pollak, Overcoming drug development bottlenecks with repurposing: Repurposing biguanides to target energy metabolism for cancer treatment. *Nat. Med.* **20**, 591–593 (2014).
57. Y. Huang, H. Zhang, Effect of overexpression of VCP on gene expression during colorectal cancer progression of HCT116 cells. GEO (Gene Expression Omnibus). https://www.ncbi.nlm.nih.gov/geo/query/acc.cgi?acc=GSE201660. Accessed 19 July 2023.
58. Y. Huang, H. Zhang, Genome-wide maps of chromatin state in HCT116 cells expressing Flag-tagged VCP. GEO (Gene Expression Omnibus). https://www.ncbi.nlm.nih.gov/geo/query/acc.cgi?acc=GSE201200. Accessed 19 July 2023.